ORIGINAL ARTICLE

Asian Herpetological Research 2021, 12(4): 331–336
DOI: 10.16373/j.cnki.ahr.210016

Chemical Composition and Crystal Structure of the Eggshell of the Green Crested Lizard *Bronchocela cristatella* (Agamidae)

Kun GUO[1], Jun ZHONG[1], Li MA[2], Yongpu ZHANG[1] and Xiang JI[1*]

[1] *College of Life and Environmental Sciences, Wenzhou University, Wenzhou 325035, Zhejiang, China*
[2] *Faculty of Ecology, Lishui University, Lishui 323000, Zhejiang, China*

Abstract The majority of extant reptiles are oviparous and produce eggs with three major components: embryo, yolk, and eggshell. The eggshell is species-specific and more diverse in squamate reptiles than in other amniote taxa. Here, we study the crystal structure, chemical composition, and bonding states of the eggshell of the green crested lizard *Bronchocela cristatella*. X-ray diffractometer (XRD) analysis showed the existence of two clearly defined and distinguishable crystalline phases, aragonite and calcite. Using the XRD data and a unit cell refinement routine, we identified two sets of cell parameters: a = 4.956 Å, b = 7.965 Å, and c = 5.734 Å for the aragonite phase; a = 4.987 Å, b = 4.987 Å, and c=17.056 Å for the calcite structure. We used x-ray photoelectron spectroscopy to examine detailed elemental composition and bonding states and found that the eggshell was composed primarily of elements C, N, Ca, and O, with C, N and O bonded to various types of hybridization in the protein of the eggshell membrane. The Ca:C:O ratio for the calcium carbonate yielded a value of ~7:8:21, which is close to the expected stoichiometric value of $CaCO_3$.

Keywords agamid lizard, aragonite, calcite, crystal structure, eggshell, elemental bonding states, X-ray diffractometer, X-ray photoelectron spectroscopy

*Corresponding authors: Prof. Xiang JI, from College of Life and Environmental Sciences, Wenzhou University, Wenzhou, China, with his research focusing on physiological and evolutionary ecology of reptiles.
E-mail: jixiang@njnu.edu.cn
Received: 20 February 2021 Accepted: 30 June 2021

1. Introduction

The eggshell of oviparous vertebrates is a bi-layered biopolymer composed of an outer, inorganic layer chemically bonded to an underlying organic matrix of several layers of fibers generally referred to as eggshell membrane. Physical structure of eggshells is species-specific and more diverse in reptiles than in other amniote taxa, ranging from flexible, parchment-shelled eggs of many squamates (lizards, snakes, and amphisbaenians) to calcareous, rigid-shelled eggs of crocodilians, many geckos and turtles (Packard and DeMarco, 1991; Schleich and Kästle, 1988; Pike *et al*., 2012; Hallmann and Griebeler, 2015; Deeming, 2018). The eggshell is an important physiological structure that represents an important case of rapid, highly structured, and regulated biomineralization; this biologically self-organized material is a useful source for the development of novel biocompatible materials such as hydroxyapatite (Rivera *et al*., 1999; Stewart *et al*., 2009; Stewart and Ecay, 2010; Campos-Casal *et al*., 2020).

The mineral composite in eggshells of amniotes exists as pure calcium carbonate ($CaCO_3$) in the form of calcite, but two other polymorphs (aragonite and vaterite, both are more soluble than calcite; Falini *et al*., 2007) of $CaCO_3$ have also been found in eggshells of reptiles (Packard *et al*., 1982; You *et al*., 1993; Wang *et al*., 2014) and birds (Board and Perrott, 1979; Portugal *et al*., 2018). The calcareous shell of turtle eggs is aragonitic (Packard *et al*., 1982; Packard and Hirsch, 1986; Packard and DeMarco, 1991; You *et al*., 1993; Deeming, 2018), whereas the eggshell of crocodilians (Ferguson, 1982), squamates (Osborne and Thompson, 2005; Wang *et al*., 2014) and birds (Stapane *et al*., 2020; see also Portugal et al., 2018) is mainly calcitic. Both calcite and aragonite morphs co-exist in the eggshell of the green sea turtle *Chelonia mydas*, as revealed by scanning electron microscopy (Baird and Solomon, 1979). The organic matrix has

nucleation sites to initiate crystal deposition on the eggshell and acts as a model for the inorganic crystal lattice-structure.

The eggshell is not merely a "container" that separates the developing embryo from the environment, but also plays a key role in modulating the exchange of water and gases between the egg and its environment (Ji and Zhang, 2001; Booth and Yu, 2008; Zhao *et al*., 2013; Tang *et al*., 2018; Stapane *et al*., 2020), and in serving as a source of calcium during embryonic development (Ji and Braña, 1999; Lu *et al*., 2009; Stewart *et al*., 2009, 2019; Stewart and Ecay, 2010; Wang *et al*., 2014). The allocation of the calcium resource, not just to the egg yolk, but also the shell, is a fine example of parental provisioning of mineral resource to offspring (Packard and Packard, 1986, 1989; Ji and Braña, 1999; Du *et al*., 2001; Cai *et al*., 2007; Lu *et al*., 2009). Given that the success of egg incubation is dependent on the physiological role of the shell and its multiple functions such as an effective barrier against pathogens and a selective biofilter, it follows that an understanding of the shell's physical structure, chemical composition and bonding states at the atomic level could elucidate adaptive value of eggshell structure and organization that defines a species ecology (Packard and DeMarco, 1991; Benton, 2005; Osborne and Thompson, 2005; Hallmann and Griebeler, 2015; Campos-Casal *et al*., 2020).

Studies on eggshell structure of reptiles have been focused mainly on shell crystal morphology, elemental composition, and/or heavy metal distribution associated with environmental pollution, the organic matrix, and bioprocessing strategy of shell mineralization (You *et al*., 1993; Sim and Nakai, 1994; Sahoo *et al*., 1996a, b; Wang *et al*., 2014). However, despite the important contribution of the shell to embryogenesis and successful incubation (Deeming and Ferguson, 1991), our knowledge on the chemical organization of the shell structure at the atomic level, in particular the binding energy of various bonds in the calcareous shell and the underlying proteinaceous shell membrane, is limited. There has been no previous study on binding energies of chemical bonds in reptilian eggshell. In this study, we used an X-ray photoelectron spectroscopy and an X-ray diffractometer to elucidate the chemical composition, crystalline structure, and the binding energy of the constituent elements in the eggshell of the green crested lizard *Bronchocela cristatella* (Agamidae). This arboreal lizard exists throughout Southeast Asia; it usually lays a clutch of two or three long, fusiform, soft-shelled eggs (Diong and Lim, 1998).

2. Materials and Methods

2.1. Eggshell samples for structural analyses Eggs of *B. cristatella* used in this study were obtained from five gravid females collected in June 2001 on Dioman Island in Malaysia. Five freshly-laid eggs, one from each clutch, were rinsed with distilled water to remove oviductal contents on the shell. Eggs were dissected to remove egg contents and their inner shell membranes were rinsed with distilled water to remove traces of yolk or albumen. Eggshells were lyophilized to a constant mass and stored in a dessicator for later use. In order to make accurate measurements of the chemical structure and binding energies, the eggshells were softened for 24 h in deionized water and cut into ~5 × 5 mm^2 pieces. Eggshell pieces were individually sandwiched between two Pyrex glass slides whose ends secured together. Flattened eggshells were oven-dried at 40 °C for 48 h prior to measurements.

2.2. Eggshell structural and lattice parameters Structure of the five eggshells was measured using a D5005 X-ray diffractometer (XRD, Siemens, Germany) at 40 kV tube voltage and 40 mA current in a θ-2θ mode with an incident X-ray wavelength of 1.540 Å (Cu Kα line). A standard XRD reference database was used to identify the specific structure of the sample. For precise lattice parameter determination, a least square fitting routine CELREF was performed for the cell refinement.

2.3. Structural composition and bonding states Elemental composition and bonding states of the five shell samples were studied by X-ray photoelectron spectroscopy (XPS) in a VG ESCALAB 220i-XL spectrometer. An Al Kα (1486.6 eV) X-ray source was used, with the analyzer set at a constant passing energy of 10 eV. The spectrometer was calibrated on the Au $4f_{7/2}$ peak at 84.00 eV. All the core-level peaks were curve fitted after Shrieley background subtraction was performed. The percentage of atomic concentrations of each element present in the sample was calculated using the peak area, the transmission function and the sensitivity factors for each of the constituent atoms. The chemical states of various bondings were determined using deconvolution techniques provided by the VG software.

2.4. Structural analyses and cell refinement Quantitative investigation of the crystalline structure of the eggshell was carried out using a D5005 X-ray diffractometer with divergence slit DS = 0.8°, anti-scattering slit AS = 1.0°, and receiving slit RS = 1.0 mm. Data were collected over a range of 15°–90°, sufficient to cover most reflections. A sample piece was mounted on a standard specimen holder, which is amorphous in nature.

2.5. X-ray photoelectron spectroscopy analysis The composition and chemical bonding states of the five shell samples were examined by XPS using an Al K (1486.6 eV) X-ray source. The usual argon ion sputter-cleaning process was not performed due to the porous nature of the eggshell. Surface clearing by ion sputtering often has an influence on the bonding configuration in the sample as was reported in Moulder *et al*. (1992).

3. Results and Discussion

3.1. X-ray diffraction pattern of eggshell crystalline structure Examination of the XRD pattern of a typical eggshell sample revealed that the shell was of polycrystalline structure with a high degree of crystallization (Figure 1). We used the crystallography database of American Society for Testing and Materials to identify the crystalline structure of the eggshell. The presence of strong reflections corresponding to 26.3°, 33.1°, and 48.7° indicates the existence of aragonite phase of $CaCO_3$. The sharp peak at 26.3° suggests that the aragonite phase of the eggshell has a preferred orientation of (111). This peak is also the preferred orientation of orthorhombic aragonite calcium carbonate. In this structure, each C atom is bonded by three O atoms to form a flat CO_3 groups. The CO_3 groups are aligned in the same plane but point in two directions. For this phase, as the Ca is relatively large for the structure at room pressure and temperature, so the aragonite phase is metastable at the room conditions. This phase, however, is commonly observed to be a constituent of the shell structures in fresh water turtles and soft-shelled turtles (Packard *et al.*, 1982; You *et al.*, 1993).

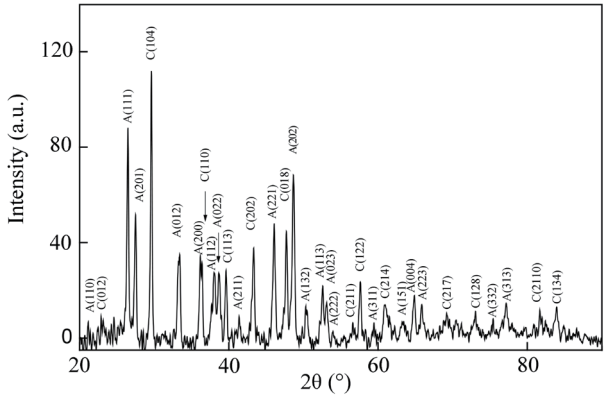

Figure 1 A typical XRD spectrum of the eggshell of *Bronchocela cristatella*, showing the co-existence of both aragonite (A) and calcite (C) phases.

In addition to the above observed aragonite phase, the XRD spectra further revealed the presence of a calcite phase as was evidenced by strong peaks at 29.6° and 43.3° (Figure 1). These peaks were due to the reflection of the (104) and (202). In the calcite phase, it could be seen that the intensity of the (104) reflection was much stronger than that of other planes (Figure 1). This phenomenon can be due to enhanced nucleation associated with the nuclear growth that is mediated by shell membrane proteins of different types during the process of biogenic crystal growth (Ronnig *et al.*, 1998), which results in an extraordinary grain growth along this direction. In this phase, the CO_3 groups are arranged in a flat triangle with C in the middle. These groups are all aligned perpendicular to the c-axis. It is remarkable to note that both aragonite and calcite phases of $CaCO_3$ crystals are present in the eggshell of *B. cristatella*. While this finding has not been previously reported for squamate reptiles (see also Wang *et al.*, 2014), our result nonetheless demonstrates that the co-occurrence of two of the three polymorphs (aragonite, calcite, and vaterite) of $CaCO_3$, is not restricted to turtles. Baird and Solomon's (1979) study on eggshells of *C. mydas* shows a X-ray pattern similar to the two-phase structure of the eggshell in this study.

3.2. Unit shell characteristics and lattice parameters When examining the aragonite and the calcite phases in the spectrum, we found a noticeable deviation between the measured peaks and standard data. A precision refinement of the unit-cell was therefore performed to find the true lattice parameters. Detailed refinement process was undertaken using a minimization software CELREF. For the aragonite phase, the structure was refined using 21 peaks, whereas for the calcite phase, only 12 peaks were used. Using the identified reflections, the minimization process yields a set of lattice parameters for each phase of the shell. For aragonite, the routine generated values of a = 4.956 Å, b = 7.965 Å and c = 5.734 Å. The volume of a unit cell was calculated to be 226.356 $Å^3$, making this phase of the shell slightly denser than that of standard $CaCO_3$. Similar cell refinement process yielded values of a = 4.987 Å, b = 4.987 Å and c = 17.056 Å for the calcite structure. The parameter c is approximately 3 times larger than that of a and b. In this case the volume of the cell is almost 1.6 times that of aragonite. Table 1 shows the detailed refined parameters.

Table 1 Refined structural parameters of aragonite and calcite phases of $CaCO_3$ using CELREF. *V* is equilibrium volume of the unit cell.

Parameter	Aragonite	Calcite
a (Å)	4.96	4.99
b (Å)	7.975	4.99
c (Å)	5.73	17.06
V ($Å^3$)	226.35	422.48
c/a	1.16	3.42

Applying the refined cell parameters, the d-spacings and the Miller indices were re-calculated and tabulated in Table 2. It could be clearly seen that the measured d-values agreed with the recalculated values remarkably well. The refinement process indeed improved the precision of the lattice parameters.

3.3. Bonding energy and Ca:C:O ratio Th XPS survey scan of a typical sample clearly revealed that the eggshell was composed primarily of elements C, N, Ca, and O (Figure 2). The percentage of atomic concentrations of the total elements present in the sample, calculated using the transmission

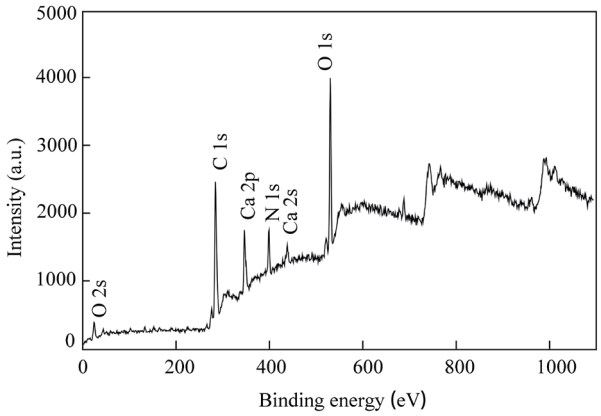

Figure 2 XPS wide scan spectra of the eggshell sample, showing the presence of elements Ca, C, N, and O.

function and the sensitivity factors for each of the constituent atoms, provided with the VG analytical software, were C = 52.5%, N = 9.8%, Ca = 6.8 %, and O = 29.8%.

Subsequent investigation on bonding state was performed using both the C 1s, N 1s, O 1s and Ca 2p photoelectron spectra. Figure 3 shows a narrow scan of C 1s, N 1s, O 1s and Ca 2p spectra, respectively. The broadness and asymmetry of the species core-level indicate the presence of multi-component peaks. The spectra were therefore fitted with Gaussian peak components mixed with Lorentzian shapes using a least squares routine, after Shirley background subtraction.

The result of peak fitting performed on C 1s spectrum yields four peaks, located at binding energy (BE) = 284.6 eV (FWHM 1.6eV), 285.6 eV (FWHM 1.5eV), 287.1 eV (FWHM 2.1eV), and 288.9 eV (FWHM 2.0eV), respectively (Figure 3a). The lowest peak at 284.6 eV is due to CH species and the adventitious carbon species on the surface originated from contamination, and the second higher BE peak located at 285.6 eV is attributed to C-N bondings in proteins as suggested by Xu *at al.* (1998). The third peak with the BE at 287.1 eV is originated from the C = NH_2 in arginine, and the last one at 288.9 eV is due to the C-O bonding in calcium carbonate. Similar three peaks have also been observed in artificial synthesis of modified carbon nitride materials (Xu *et al.*, 1998).

For the N 1s, however, the broadness (FWHM of 2.7 eV) and asymmetry of the spectrum showing in Figure 3b implies that the N curve consists of several overlapping peaks. Fitting routine yielded three decomposed peaks located at BE = 398.8 eV (FWHM 1.8 eV), 399.6 eV (FWHM 1.7 eV) and 401.2 eV (FWHM 1.6 eV), respectively. The first peak at 398.8 eV is attributed to nitrogen atoms having two carbon neighbors in protein whereas the contribution at 399.6 eV is asssigned to the cyanogroup (-C≡N) which often exists at room temperatures in protein. The third peak is attributed to N-O bondings in various proteins. Peaks corresponding to atomic N (BE = 409.9 eV) were not observed in the N 1s spectrum, which implies that all N atoms in the shell were indeed bonded to other atoms.

Table 2 XRD data for the sample under investigation, showing expected and calculated *d*-spacings and the crystal indices.

Aragonite			Calcite		
(h k l)	*d-exp* (Å)	*d-cal* (Å)	(h k l)	*d-exp* (Å)	*d-cal* (Å)
1 1 0	4.204	4.207	0 1 2	3.863	3.860
1 1 1	3.384	3.392	1 0 4	3.022	3.035
0 2 1	3.251	3.270	1 1 0	2.483	2.495
0 1 2	2.699	2.697	1 1 3	2.275	2.285
2 0 0	2.491	2.480	2 0 2	2.088	2.090
1 1 2	2.369	2.369	2 1 1	1.624	1.626
0 2 2	2.323	2.326	1 2 2	1.599	1.604
2 1 1	2.183	2.186	2 1 4	1.523	1.525
2 2 1	1.971	1.975	2 1 7	1.357	1.356
2 0 2	1.871	1.874	1 2 8	1.295	1.297
1 3 2	1.814	1.813	2 1 10	1.181	1.180
1 1 3	1.741	1.740	1 3 4	1.153	1.154
0 2 3	1.723	1.723			
2 2 2	1.698	1.696			
3 1 1	1.555	1.556			
1 5 1	1.467	1.466			
0 0 4	1.437	1.434			
2 2 3	1.417	1.415			
3 3 2	1.260	1.260			
3 1 3	1.235	1.235			
1 5 3	1.188	1.188			

The O 1s spectra can be used to further substantiate the interpretation of the above data. The spectra in Figure 3c show two components at 530.5 and 531.4 eV, which testify bonded O atoms to C in the form N≡C = O in proteins and C–O in $CaCO_3$. Figure 3d shows the binding energy of Ca 2p. The doublet characteristics of the Ca 2p is clearly seen. From this spectrum, we found that all Ca atoms were bonded with CO3 group with the binding energy of 346.8 eV (Figure 3d). Using the peak areas of the Ca 2p, C 1s and O 1s spectra, the Ca:C:O ratio calculated from the deconvoluted components for calcium carbonate yields a value of 7:8:21. It is remarkable that the ratio of Ca:C:O of the shell sample is close to the expected stoichiometric value of $CaCO_3$.

4. Conclusions

In this study, we used XRD and XPS techniques to investigate the structure and chemical state of the eggshell of *B. cristatella*. A dual $CaCO_3$ phase (calcite and aragonite) was found in the eggshell of this lizard. Previous work reports this chemical phenomenon from turtle eggshells only (Deeming, 2018). Using the refinement technique, we identified two sets of lattice parameters. Recalculation of the reflections revealed remarkable agreement between the experimentally measured peaks and the calculated values. Measurements of chemical

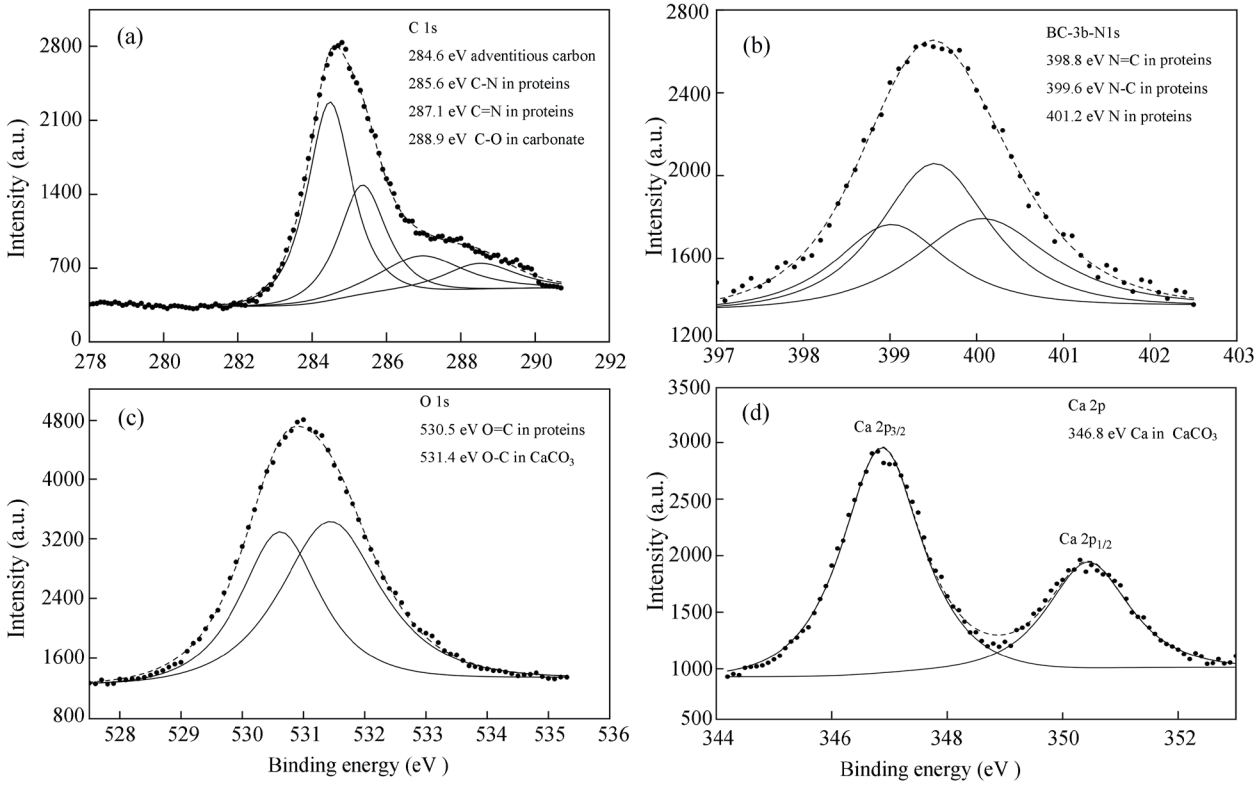

Figure 3 XPS core-level spectra for (a) C 1s, (b) N 1s, (c) O 1s, and (d) Ca 2p in an eggshell sample of *Bronchocela cristatella*.

composition revealed that the eggshell of *B. cristatella* consists mainly of elements Ca, C, N, and O. Various bonding states were identified and a near stoichiometric value of $CaCO_3$ was obtained. Significant amounts of chemical bonds were found in between carbon, nitrogen and oxygen in the proteins of the shell membrane. Further work could usefully test whether the dual $CaCO_3$ phase offers reproductive and/or protective advantages. In *Crotophaga major*, a communally nesting bird, vaterite may act as a shock absorber protecting the underlying calcite shell from mechanical damage caused by collision with other eggs and reducing the risk of eggshell fracture during incubation (Portugal *et al.*, 2018).

Acknowledgments We thank Cheong-Hoong DIONG for arranging animal collection in Malaysia, and Ling ZHANG for collecting and preparing eggshell specimens.

References

Baird T., Solomon S. E. 1979. Calcite and aragonite in the eggshell of *Chelonia mydas* L. J Exp Mar Biol Ecol, 36: 295–303

Benton M. J. 2005. Vertebrate Palaeontology. 3rd Edition. Oxford, UK: Blackwell Publishing

Board R. G., Perrott H. R. 1979. Vaterite, a constituent of the eggshells of the non-parasitic cuckoos, *Guira guira* and *Crotophagi ani*. Calcif Tissue Int, 29: 63–69

Booth D. T., Yu C. Y. 2008. Influence of the hydric environment on water exchange and hatchlings of rigid-shelled turtle eggs. Physiol Biochem Zool, 82: 382–387

Cai Y., Zhou T., Ji X. 2007. Embryonic growth and mobilization of energy and material in oviposited eggs of the red-necked keelback, *Rhabdophis tigrinus lateralis*. Comp Biochem Physiol A, 147: 57–63

Campos-Casal F. H., Cortez F. A., Gomez E. I., Chamut S. N. 2020. Chemical composition and microstructure of recently oviposited eggshells of *Salvator merianae* (Squamata: Teiidae). Herpetol Conser Biol, 5: 341–359

Deeming D. C. 2018. Nesting environment may drive variation in eggshell structure and egg characteristics in the Testudinata. J Exp Zool A, 147: 57–63

Deeming D. C., Ferguson M. W. J. 1991. Gas exchange across reptilian eggshells. In Deeming D. C., Ferguson M. W. J. (Eds.), Egg Incubation: Its Effects on Embryonic Development in Birds and Reptiles. Cambridge: Cambridge University Press, 277–283

Diong C.-H., Lim S. S. L. 1998. Taxonomic review and morphometric description of *Bronchocela cristatella* (Kuhl, 1820) (Squamata: Agamidae) with notes on other species in the genus. Raffles B Zool, 46: 345–359

Du W.-G., Ji X., Xu W.-Q. 2001. Dynamics of material and energy during incubation in the soft-shelled turtle (*Pelodiscus sinensis*). Acta Zool Sin, 47: 371–375

Falini G., Manara S., Fermani S., Roveri N., Goisis M., Manganelli G., Cassar L. 2007. Polymeric admixtures effects on calcium carbonate crystallization: Relevance to cement industries and biomineralization. CrystEngComm, 9: 1162–1170

Ferguson M. W. J. 1982. The structure and composition of the eggshell and embryonic membranes of *Alligator mississippiensis*. Trans Zool Soc Lond, 36: 99–152

Hallmann K., Griebeler E. M. 2015. Eggshell types and their evolutionary

correlation with life-history strategies in squamates. PLoS One, 10: e0138785

Ji X., Braña F. 1999. The influence of thermal and hydric environments on incubating eggs and embryonic use of energy and nutrients in the wall lizard *Podarcis muralis*. Comp Biochem Physiol A, 124: 205–213

Ji X., Zhang C.-H. 2001. Effects of thermal and hydric environments on incubating eggs, hatching success and hatchling traits in the Chinese skink (*Eumeces chinensis*). Acta Zool Sin, 47: 256–265

Lu H.-L., Hu R.-B., Ji X. 2009. Embryonic growth and mobilization of energy and material during incubation in the checkered keelback snake, *Xenochrophis piscator*. Comp Biochem Physiol A, 152: 214–218

Moulder J. F., Stickle W. F., Sobol P. E., Bomben K. D. 1992. Handbook of X-ray Photoelectron Spectroscopy, Physical Electronics, Inc. Minnesota, USA

Osborne L., Thompson M. B. 2005. Chemical composition and structure of the eggshell of three viviparous lizards. Copeia, 2005: 683–692

Packard M. J., DeMarco V. G. 1991. Eggshell structure and formation in eggs of oviparous reptiles. In Deeming D. C., Ferguson M. W. J. (Eds.), Egg Incubation: Its Effects on Embryonic Development in Birds and Reptiles. Cambridge: Cambridge University Press, 53–69

Packard M. J., Hirsch K. E. 1986. Scanning electron microscopy of eggshells of contemporary reptiles. Scan Electron Microsc, 4: 1581–1590

Packard M. J., Packard G. C. 1986. The effect of water balance of eggs on growth and calcium metabolism of embryonic painted turtles (*Chrysemys picta*). Physiol Zool, 59: 398–405

Packard M. J., Packard G. C. 1989. Mobilization of calcium, phosphorus, and magnesium by embryonic alligators (*Alligator mississippiensis*). Am J Physiol R, 257: 15411547

Packard M. J., Packard G. C., Boardman T. M. 1982. Structure of eggshells and water relations of reptilian eggs. Herpetologica, 38: 136–155

Pike D. A., Andrews R. M., Du W.-G. 2012. Eggshell morphology and gekkotan life-history evolution. Evol Ecol, 26: 847–861

Portugal S. J., Bowen J., Riehl C. 2018. A rare mineral, vaterite, acts as a shock absorber in the eggshell of a communally nesting bird. Ibis, 160: 173–178

Rivera E. M., Araiza M., Brostow W., Castano V. M., Diaz-Estrada J. R., Hernandez E. R., Rodriguez J. R. 1999. Synthesis of hydroxyapatite from eggshells. Mater Lett, 41: 128–134

Ronnig C., Feldermann R., Merk R., Hofass H., Reinke P., Thiele J. U. 1998. Carbon nitride deposited using energetic species: A review on XPS studies. Phys Rev B, 58: 2207–2215

Sahoo G., Mohapatra B. K., Sahoo R. K., Mohanty-Hejmadi P. 1996a. Ultrastructure and characteristics of eggshells of the olive ridley turtle (*Lepidochelys olivacea*) from Gahirmatha, India. Acta Anat, 156: 261–267

Sahoo G., Sahoo R. K., Mohanty-Hejmadi P. 1996b. Distribution of heavy metals in the eggs and hatchlings of olive ridley sea turtle, *Lepidochelys olivacea*, from Gahirmatha, Orissa. Indian J Mar Sci, 25: 371–372

Schleich H. H., Kästle W. 1988. Reptile Eggshells SEM Atlas. Stuttgart: Gustav Fischer

Sim J. S., Nakai S. 1994. Egg uses and processing technologies: New developments. CAB International Oxon, UK

Stapane L, Le Roy N, Ezagal J, Rodriguez-Navarro A. B., Labas V., Combes-Soia L., Hincke M. T., Gautron J. 2020. Avian eggshell formation reveals a new paradigm for vertebrate mineralization via vesicular amorphous calcium carbonate. J Biol Chem, 295: 15853–15869

Stewart J. R., Ecay T. W. 2010. Patterns of maternal provision and embryonic mobilization of calcium in oviparous and viviparous squamate reptiles. Herpetol Conser Biol, 5: 341–359

Stewart J. R., Ecay T. W., Heulin B. 2009. Calcium provision to oviparous and viviparous embryos of the reproductively bimodal lizard *Lacerta* (*Zootoca*) *vivipara*. J Exp Biol, 212: 2520–2524

Stewart J. R., Pyles R. A., Mathis K. A., Ecay T. W. 2019. Facultative mobilization of eggshell calcium promotes embryonic growth in an oviparous snake. J Exp Biol, 222: jeb193565

Tang W. Q., Zhao B., Chen Y., Du W. G. 2018. Reduced egg shell permeability affects embryonic development and hatchling traits in *Lycodon rufozonatum* and *Pelodiscus sinensis*. Integr Zool, 13: 58–69

Wang Z., Lin L. H., Ji X. 2014. Unhatched and hatched eggshells of the Chinese cobra *Naja atra*. Asian Herpetol Res, 5: 276–280

Xu S. Y., Li H. S., Li Y. A., Lee S., Huan C. H. A. 1998. On the structure and composition of polycrystalline carbon nitride films synthesized by reactive rf magnetron sputtering. Chem Phys Lett, 287: 731–736

You W. H., Wang P. C., Hua Y. 1993. On the structure of shells from eggs of *Chinemys reevesii*. J East China Normal Univ (Nat Sci), 1993(2): 99–105

Zhao B., Chen Y., Wang Y., Ding P., Du W.-G. 2013. Does the hydric environment affect the incubation of small rigid-shelled turtle eggs? Comp Biochem Physiol A, 164: 66–70

Handling Editor: Chen YANG

How to cite this article:

Guo K., Zhong J., Ma L., Zhang Y. P., Ji. X. Chemical Composition and Crystal Structure of the Eggshell of the Green Crested Lizard *Bronchocela cristatella* (Agamidae). Asian Herpetol Res, 2021, 12(4): 331–336. DOI: 10.16373/j.cnki.ahr.210016